Pulmonary inflammation impacts on CYP1A1-mediated respiratory tract DNA damage induced by the carcinogenic air pollutant benzo[*a*]pyrene

Volker M. Arlt[*,1], Annette M. Krais[*], Roger W. Godschalk[†], Yanira Riffo-Vasquez[‡], Iveta Mrizova[§], Candice A. Roufosse[¶], Charmaine Corbin[*], Shi Quan[†], Eva Frei[#], Marie Stiborova[§], Frederik-Jan van Schooten[†], David H. Phillips[*], and Domenico Spina[‡]

[*]Analytical and Environmental Sciences Division, MRC-PHE Centre for Environment & Health, King's College London, London SE1 9NH, United Kingdom, [†]Department of Toxicology, School for Nutrition, Toxicology and Metabolism (NUTRIM), Maastricht University Medical Centre, 6200 MD Maastricht, The Netherlands, [‡]Sackler Institute of Pulmonary Pharmacology, Institute of Pharmaceutical Science, King's College London, London SE1 9NH, United Kingdom, [§]Department of Biochemistry, Faculty of Science, Charles University, 12840 Prague 2, Czech Republic, [¶]Department of Histopathology, Imperial College Healthcare NHS Trust, Hammersmith Hospital, London W12 0HS, United Kingdom, [#]Division of Preventive Oncology, National Center for Tumor Diseases, German Cancer Research Center (DKFZ), Im Neuenheimer Feld 280, 69120 Heidelberg, Germany

[1]To whom correspondence should be addressed at Analytical and Environmental Sciences Division, MRC-PHE Centre for Environment & Health, King's College London, Franklin-Wilkins Building, 150 Stamford Street, London SE1 9NH, United Kingdom, Tel: +44-207-848-3781, E-mail: volker.arlt@kcl.ac.uk.

ABSTRACT

Pulmonary inflammation can contribute to the development of lung cancer in humans. We investigated whether pulmonary inflammation alters the genotoxicity of polycyclic aromatic hydrocarbons (PAHs) in the lungs of mice and what mechanisms are involved. To model non-allergic acute inflammation, mice were exposed intranasally to lipopolysaccharide (LPS; 20 μg/mouse) and then instilled intratracheally with benzo[*a*]pyrene (BaP; 0.5 mg/mouse). BaP-DNA adduct levels, measured by ^{32}P-postlabelling analysis, were ~3-fold higher in the lungs of LPS/BaP-treated mice than in mice treated with BaP alone. Pulmonary Cyp1a1 enzyme activity was decreased in LPS/BaP-treated mice relative to BaP-treated mice suggesting that pulmonary inflammation impacted on BaP-induced Cyp1a1 activity in the lung. Our results showed that Cyp1a1 appears to be important for BaP detoxification *in vivo* and that the decrease of pulmonary Cyp1a1 activity in LPS/BaP-treated mice results in a decrease of pulmonary BaP detoxification, thereby enhancing BaP genotoxicity (*i.e.* DNA adduct formation) in the lung. Because less BaP was detoxified by Cyp1a1 in the lungs of LPS/BaP-treated mice, more BaP circulated via the blood to extra-pulmonary tissues relative to mice treated with BaP only. Indeed, we observed higher BaP-DNA adduct levels in livers of LPS/BaP-treated mice compared to BaP-treated mice. Our results indicate that pulmonary inflammation could be a critical determinant in the induction of genotoxicity in the lung by PAHs like BaP. Cyp1a1 appears to be involved in both BaP bioactivation and detoxification although the contribution of other enzymes to BaP-DNA adduct formation in lung and liver under inflammatory conditions remains to be explored.

Keywords: benzo[*a*]pyrene, pulmonary inflammation, cytochrome P450, carcinogen metabolism, DNA adducts, bronchoalveolar lavage.

INTRODUCTION

Globally, lung cancer is the leading cause of cancer death. Tobacco smoking is the overwhelming cause of lung cancer, although vehicle engine exhaust (*e.g.* diesel exhaust) and ambient air pollution are also implicated (IARC, 2013; Loomis *et al.*, 2013). Inflammatory diseases of the lung, including fibrosis and chronic obstructive pulmonary disease (COPD), are associated with higher lung cancer risk (Brody and Spira, 2006; Schottenfeld and Beebe-Dimmer, 2006). Lung cancer risk in smokers with COPD is increased up to 10-fold in comparison to smokers without COPD (Brody and Spira, 2006). Many inflammatory agents can contribute to the development of diseases like COPD or asthma, including inhaled combustion derived particles such as cigarette smoke, ambient air particulate matter and diesel exhaust particles (Kelly and Fussell, 2011). Inhalation of such particles can cause a local pulmonary response which is characterised by the influx of neutrophils into the airways (Knaapen *et al.*, 2006). In contrast to their innate protective role in immunity, neutrophils contribute to the pathogenesis of inflammatory lung diseases like COPD and promote tumour development (Grivennikov *et al.*, 2010; Knaapen*et al.*, 2006).

A number of studies have found that occupational exposure to diesel exhaust leads to increased risk of lung cancer (Attfield *et al.*, 2012; Silverman *et al.*, 2012) and the International Agency for Research on Cancer (IARC) has classified diesel engine exhaust as carcinogenic to humans (Group 1) (IARC, 2013). However, the mechanism of diesel carcinogenesis and precise identity of the carcinogenic components of diesel exhaust are still incompletely understood, as is the magnitude of the carcinogenic risk from environmental exposure. Although exposure to diesel exhaust material induces pulmonary inflammation and exacerbates chronic respiratory inflammatory conditions (Kelly and Fussell, 2011), the contribution of such inflammation to diesel exhaust associated carcinogenic risk potential has not been examined in any great detail. By analogy with the causation of lung cancer by

tobacco smoking (Walser *et al.*, 2008) it was therefore the aim of this study to examine how inflammation in the lung alters the genotoxicity of polycyclic aromatic hydrocarbons (PAHs), which occur in the particulate phase of diesel exhaust, and what specific mechanisms are involved.

PAHs such as benzo[*a*]pyrene (BaP), also an IARC Group 1 carcinogen (IARC, 2010), exert their carcinogenic effects only after metabolic activation. As shown in Figure 1 BaP is activated by cytochrome P450 (CYP) enzymes, CYP1A1 and CYP1B1 being the most important isoenzymes (Baird *et al.*, 2005), resulting in highly reactive diol-epoxides capable of forming covalent DNA adducts that can lead to mutations through errors in DNA replication (Phillips, 2005). Inflammatory reactions *in vivo* involve the production and release of a range of signalling molecules including cytokines and chemokines (Grivennikov *et al.*, 2010; Schwarze *et al.*, 2013). *In vitro* experiments have shown that cytokines like tumour necrosis factor-α (TNF-α) formed after environmental exposures can alter the expression of metabolic enzymes such as CYPs (*e.g.* CYP1A1, CYP1B1) involved in BaP bioactivation (Umannova *et al.*, 2008; Smerdova *et al.*, 2014). Other *in vitro* studies have revealed that neutrophil-derived myeloperoxidase (MPO) can activate the BaP metabolite BaP-7,8-dihydrodiol to reactive species (*i.e.* BaP-7,8-dihydrodiol-9,10-epoxide [BPDE]) that form DNA adducts in lung cells (Petruska *et al.*, 1992; Borm *et al.*, 1997).

In the present study we investigated whether lung inflammation alters the capacity for diesel exhaust carcinogens like BaP to cause DNA damage (*e.g.* DNA adducts) *in vivo* and the mechanisms involved. To model non-allergic acute inflammation, mice were exposed to lipopolysaccharide (LPS) and then instilled with BaP. DNA adduct formation was determined by ^{32}P-postlabelling analysis.

MATERIALS AND METHODS

Carcinogen. Benzo[*a*]pyrene (BaP; purity ≥96%) was obtained from Sigma Aldrich.

Animal treatment. C57B16 mice (male; ~8-10 weeks old, 20-25 g) were obtained from Charles River Laboratories. All animal experiments were carried out at King's College London under license according to protocols approved by the Home Office under 'The Animals (Scientific Procedures) Act (1986)' after approval by the institutional ethics committee. Animals were kept under controlled pathogen-free conditions and allowed food and water *ad libitum*. In total, four groups of mice (n = 4 per experiment; repeated in triplicate; n = 12 in total) were used as follows (see Fig. 2): Group I: mice were instilled nasally with saline and 24 hours later instilled intratracheally with vehicle, tricaprylin (25 µL/mouse). Group II: to induce acute pulmonary inflammation mice received an intranasal dose of 20 µg lipopolysaccharide (LPS; *Escherichia coli*, serotype O55:B5; 1 mg/mL; Sigma), and 24 hours later they received tricaprylin (25 µL/mouse) by intratracheal instillation. Group III: mice were instilled nasally with saline and 24 hours later instilled intratracheally with BaP (0.5 mg BaP dissolved in 25 µL tricaprylin). Group IV: mice received an intranasal administration of 20 µg LPS followed 24 hours later with BaP (0.5 mg BaP/mouse) by intratracheal instillation. In order to have sufficient material available for histopathology and several biological assays, experiments were performed in triplicate on separate occasions (3×n = 4/group). All instillations were performed under anaesthesia with isoflurane (Sigma) following injection with ketamine/zylazine (1 mg/0.166 mg per mouse, respectively; Sigma). Mice were killed 3 days after exposure after anaesthesia with 2 g/kg body weight urethane (Sigma) by intraperitoneal administration and a cannula was inserted into the exposed trachea. For the collection of inflammatory cells by bronchoalveolar lavage (BAL) three 0.5-mL aliquots of sterile saline were injected into the lungs. Lung and liver

tissue were also collected, snap-frozen in liquid nitrogen and stored at –80ºC until analysis. For histopathology lung sections were fixed for 48 hours in PBS containing 4% paraformaldehyde.

Assessment of the pulmonary inflammation by histopathology and BAL analysis. Fixed lung sections were embedded in paraffin and 7-micron sections were cut and stained with haematoxylin-eosin (H&E) (Arlt *et al.*, 2011). Slides were randomized and analysed at 10× magnification for the number of fields with inflammation, expressed as % of the total number of fields of lung tissue on the section. At 40× magnification, inflammation was qualified as either predominantly neutrophilic or predominantly monocytic.

From the collected BAL fluid, a 50-µL aliquot was added to 50 µL of haemolysis (Turk) solution. The total number of cells in the BAL fluid was counted with an improved Neubauer haemocytometer. For differential cell counts, cytospin preparations were prepared from aliquots of BAL fluid (100 µL), centrifuged at 250 g for 1 min using a Shandon Cytospin 2 (Shandon Southern Instruments, Sewickley, PA, USA) at room temperature and stained with Diffquick. Two hundred cells were counted to determine the proportion of neutrophils, eosinophils and monocytes using standard morphological criteria (Holand *et al.*, 2014).

Detection of DNA adducts. DNA from tissue was isolated by a standard phenol-chloroform extraction method. DNA adduct analysis was performed by the nuclease P1 enrichment version of the ^{32}P-postlabelling method as described previously (Phillips and Arlt, 2007; Phillips and Arlt, 2014) with minor modifications. DNA samples (4 µg) were digested with micrococcal nuclease (288 mU; Sigma) and calf spleen phosphodiesterase (1.2 mU; MP Biomedical), and then enriched and labelled as reported. Resolution of ^{32}P-labelled adducts

was performed by polyethyleneimine-cellulose (PEI) thin-layer chromatography (TLC) (Arlt *et al.*, 2008). After chromatography TLC plates were scanned using a Packard Instant Imager (Dowers Grove, IL, USA). DNA adduct levels (RAL, relative adduct labelling) were calculated from adduct counts per minute (cpm), the specific activity of [γ-^{32}P]ATP and the amount of DNA (pmol) used. Results were expressed as DNA adducts/10^8 normal nucleotides (nt). An external BPDE-modified DNA standard was used to identify BaP-DNA adducts.

Preparation of pulmonary and hepatic microsomal and cytosolic samples. Pooled pulmonary and hepatic microsomal and cytosolic fractions (n = 4) were isolated as described (Arlt *et al.*, 2008; Martin *et al.*, 2010). Briefly, tissue samples were pulverized by grinding snap-frozen pooled lung or liver specimens in a Teflon container frozen in liquid nitrogen with a steel ball using a dismembrator (2600 UPM for 30 seconds; Braun Melsungen AG, Germany). The frozen tissue powder was then homogenized by hand in 0.067 M potassium phosphate buffer (pH 7.4) with 0.5% potassium chloride in a Potter-Elvehjem glass-Teflon homogenizer. The buffer volume (in µL) used was three times the weight (in mg) of the organ. Nuclei and debris were removed by centrifugation at 18,000 *g* for 30 minutes at 4ºC. From the supernatant, microsomal pellets were obtained at 100,000 *g* after 1 hour. Supernatant (cytosolic fraction) was gently levered off the sediment into 200-µL aliquots and stored at −80°C until further analysis. The sediment (microsomal fraction) was resuspended in phosphate buffer (lung in approximately the same volume (in µL) as their weight (in mg), liver in twice their weight) and small aliquots (100 µL) were stored at −80°C until further analysis. Protein concentrations in cytosolic and microsomal fractions were measured using the bicinchoninic acid (BCA) protein assay with bovine serum albumin as a standard.

Expression of pulmonary and hepatic Cyp1 protein. Immunoquantitation of Cyp1a1 and Cyp1b1 in microsomal fractions was carried out by sodium dodecyl sulphate (SDS)-10% polyacrylamide gel electrophoresis of samples containing 30 μg microsomal proteins. After migration, proteins were transferred onto polyvinylidenedifluoride membranes. Mouse Cyp1a1 protein was probed with goat-anti rat CYP1A1 polyclonal antibodies (1:2500, Antibodies-online GmbH, Aachen, Germany) as reported elsewhere (Stiborova *et al.*, 2014). The goat-anti rat CYP1A1 antibodies recognise this enzyme in mouse pulmonary and hepatic microsomes as one protein band. Rat recombinant CYP1A1 (in Supersomes™, Gentest Corp., Woburn, MA, USA) was used as positive controls to identify the band of Cyp1a1 in murine microsomes. Mouse Cyp1b1 protein was probed with rabbit-anti human CYP1B1 polyclonal antibodies (G-25) (1:200, Santa Cruz Biotechnology, Dallas, Texas, USA). The goat-anti rabbit CYP1B1 antibodies recognise this enzyme as one protein band. Human recombinant CYP1B1 (in Supersomes™) was used as positive control. The antigen–antibody complex was visualized with an alkaline phosphatase-conjugated rabbit anti-chicken IgG antibody and 5-bromo-4-chloro-3-indolylphosphate/nitrobluetetrazolium as chromogenic substrate (Stiborova *et al.*, 2006). Glyceraldehyde phosphate dehydrogenase was used as loading control and detected by its antibody (1:750, Millipore; MA, USA). Band intensity was quantified using the GeneTools software.

Measurement of pulmonary and hepatic Cyp1a enzyme activity. Microsomal Cyp1a enzyme activity (measured as relative fluorescence unit [RFU]/minute) was determined by following the conversion of 7-ethoxyresorufin into resorufin (EROD assay) using fluorescent measurement on a Synergy HT Plate Reader (Bio-TEK Instruments, USA; 530 nm excitation, 580 nm emission) (Mizerovska *et al.*, 2011). Cyp1a enzyme activity (measured as RFU/ minute) was also measured with 3-cyano-7-ethoxycoumarin (CEC) as substrate (Martin *et al.*,

2010). Briefly, in a 96-well plate the incubation mixture (200 µL) contained 67 mM potassium phosphate buffer (pH 7.4), 9 mM glucose-6-phosphate, 0.9 U glucose-6-phosphate dehydrogenase, 4.5 mM magnesium chloride, 0.9 mM NADP, 5 µM CEC (dissolved in DMSO) and 50 µg of microsomal fraction. The reaction was initiated by the addition of CEC and the formation of 3-cyano-7-hydroxycoumarin was measured every 2 minutes for 30 minutes (409 nm excitation, 460 nm emission).

Measurement of pulmonary and hepatic Nqo1 enzyme activity. Nqo1 enzyme activity in cytosolic samples was measured with menadione (2-methyl-1,4-naphthoquinone) as substrate essentially as described previously (Mizerovska*et al.*, 2011). The standard assay system in a 24-well plate contained in 1 mL (final concentration) 25 mM Tris-HCl (pH 7.5), 0.12 % bovine serum albumin, 200 µM NADH, 10 µM menadione (dissolved in methanol), 77 µM cytochrome *c* and 50 µg of cytosolic fraction. The reaction was initiated by the addition of the cytosolic fraction. Enzyme activity (measured as RFU/min) was determined by following the conversion of cytochrome *c* at 550 nm on a Synergy HT Plate Reader.

Expression of Cyp1b1 gene expression in the lung. Gene expression analysis was essentially performed as described (Krais *et al.*, 2015). Briefly, RNA was isolated from lung samples using the GenElute Mammalian Total RNA Mini Prep Kit (Sigma, UK) according to the manufacturer's instruction. Reserve transcription was performed using random primers and SuperScript® III Reserve Transcriptase (Life Technologies, UK) RNA expression was analysed by quantitative real-time polymerase chain reaction (qRT-PCR) using TaqMan® Universal PCR Master Mix (Life Technologies) and TaqMan® gene expression primers according to the manufacturer's protocol with a 7500HT Fast Real Time PCR System (Applied Biosystems, UK). Probe (Life Technologies, UK) *Cyp1b1*-Mm00487229_m1 was

used and expression levels were normalised to housekeeping gene *Gapdh* (4352341E). Relative gene expression was calculated using the comparative threshold cycle (C_T) method (Kucab *et al.*, 2012).

Measurement of nucleotide excision repair (NER) capacity. The ability of NER-related enzymes present in isolated tissue extracts to detect and incise substrate DNA containing BPDE-DNA adducts was measured using a modified comet assay (Langie *et al.*, 2006). Tissue protein extracts were prepared as described previously (Gungor *et al.*, 2010a), and protein concentrations were optimised for analysis of lung and liver samples (0.2 mg/mL). The *ex vivo* repair incubation and electrophoresis were performed according to the published protocol (Langie *et al.*, 2006). Dried slides stained with ethidium bromide (10 µg/mL) were viewed with a Zeiss Axioskop fluorescence microscope. Comets were scored using the Comet III system (Perceptive Instruments, UK). Fifty nucleoids were assessed per slide and each sample was analysed in duplicate. All samples were measured blindly. Tail intensity (% tail DNA) was used to calculate repair capacity of the tissue extracts (Langie *et al.*, 2006).

Statistical analysis. Statistical analyses were performed with Prism GraphPad Software and $P < 0.05$ was considered significant.

RESULTS

Pulmonary histopathology

Pulmonary inflammation three days after exposure to LPS was assessed by H&E staining (Fig. 3). The semi-quantitative assessment is summarised in Table 1. The bronchi and vessels in all groups appeared unaffected. In all four groups, there were foci of alveolar inflammation (pneumonia), but the size of the foci and the composition of inflammatory cells were different. Controls (Group I) showed few inflammatory foci (5-14% of fields), which were small in size and composed predominantly of neutrophils. LPS-treated animals (Group II) showed an increase in inflammatory foci (26-92% of fields) as loose collections mainly of macrophages extending over a larger area. BaP and LPS+BaP treated animals (Groups III and IV) showed an intermediate number of inflammatory foci (4-32% and 4-41% respectively), roughly of the same composition and size as seen in the LPS-treated animals (Group II).

Inflammatory response in BAL

Using morphological criteria the number of monocytes, eosinophils and neutrophils were counted in BAL fluid (Fig. 4). LPS treatment (Group II) caused significant increases in neutrophils (Fig. 4B) and mononuclear leukocytes (Fig. 4C) recruitment to the lung relative to control mice (Group I). No such effect was seen for eosinophils (Fig. 4D). The recruitment of neutrophils, used as a measure of pulmonary inflammation, in mice treated with LPS and LPS/BaPwas high (Fig. 4B). In LPS-treated mice (Group II) the number of neutrophils was ~22-fold higher than in control mice (Group I) and BaP-treated mice (Group III), however, additional treatment with BaP (Group IV) had no additional effect on neutrophil recruitment. More specifically, 2-way ANOVA showed a statistically significant effect of LPS-induced

inflammation on neutrophil recruitment [$F(1,41) = 31.11$, $P < 0.0001$] but was not affected by BaP treatment. There was no significant interaction effect.

DNA adduct formation in lung and liver

The DNA adduct pattern observed by TLC ^{32}P-postlabelling in BaP-treated mice (Groups III and IV) consisted of a single adduct spot, in both lung and liver. Although the ^{32}P-postlabelling method does not provide any structural information of the BaP-derived DNA adduct formed, using mass spectrometry the adduct formed *in vivo* was previously identified (Arlt *et al.*, 2008) as 10-(deoxyguanosin-N^2-yl)-7,8,9-trihydroxy-7,8,9,10-tetrahydro-BaP (dG-N^2-BPDE) (Fig. 1; *inserts*). DNA adducts were not detected either in control (Group I) or in LPS-treated animals (Group II). BaP-DNA adduct levels ranged from 10-30 adducts per 10^8 nucleotides (Fig. 5). Adduct levels were significantly higher in both lung (~2.5-fold) and liver (~3.5-fold) of LPS/BaP-treated mice (Group IV) than in mice treated with BaP alone (Group III).

Expression of BaP-metabolising enzymes in lung and liver

Cyp1a1 protein levels measured by Western blotting showed a ~5-fold induction in the lungs after BaP treatment (Group III) (Fig. 6A). Similarly pulmonary Cyp1a1 protein levels increased ~5-fold in LPS/BaP-treated mice (Group IV) relative to mice treated with LPS alone (Group II). Even though intensities of the Cyp1a1 protein bands in control (untreated) and LPS-treated mice were weak, a clear increase in Cyp1a1 protein levels was detectable in BaP- and LPS/BaP-treated mice. In accordance with these findings treatment of mice with BaP led to a strong increase in EROD (Fig. 7A) and CEC activity (Fig. 7B) in pulmonary microsomes. Interestingly, pulmonary Cyp1a enzyme activity was significantly lower (~2-fold) in LPS/BaP-treated mice (Group IV) than in mice treated with BaP alone (Group III).

Using Western blotting we found only a slight increase (~1.5 fold) in Cyp1a1 protein levels in the liver after BaP treatment (Group III) (Fig. 6B). Hepatic Cyp1a1 protein levels increased further in the LPS/BaP-treated mice (Group IV) relative to mice treated with BaP only (Group III). Similarly, hepatic EROD (Fig. 7C) and CEC activity (Fig. 7D) was up to ~2-fold higher in LPS/BaP-treated mice (Group IV) compared to mice treated with BaP only (Group III). In addition, LPS exposure alone let to a detectable Cyp1a1 activity in the liver with both substrates (Group II).

As BaP derivates can also be partly metabolised by NQO1, we also determined the activity of Nqo1 in mice exposed to BaP. Nqo1 activity was detected in both lung and liver cytosolic samples of all groups (Fig. 8). Nqo1 enzyme activity was higher after LPS (Group II), BaP (Group III) and LPS/BaP exposure (Group IV) relative to controls (Group I), in both lung (Fig. 8A) and liver (Fig. 8B). Interestingly, pulmonary Nqo1 enzyme activity was significantly lower in LPS/BaP-treated mice (Group IV) than mice treated with BaP alone (Group III), although the magnitude of the effect was modest (1.2-fold) (Fig. 8A). No difference in Nqo1 enzyme activity between the BaP (Group III) and LPS/BaP group (Group IV) was observed in the liver (Fig. 8B).

As previous studies have indicated that CYP1B1 may play a role in the metabolic activation of BaP within inflamed tissue (Umannova *et al.*, 2008; Smerdova *et al.*, 2013; 2014), expression of *Cyp1b1* mRNA in the lung was determined by qRT-PCR. However, as shown in Figure 9A no difference in *Cyp1b1* expression was observed between treatment groups. These results were in line with Cyp1b1 protein expression determined in pulmonary microsomes (Fig. 9B). Only very faint Cyp1b1 protein bands were detectable by Western blotting in all treatment groups (Groups I-IV) which could not be accurately quantified.

DNA repair capacity in lung and liver

We assessed whether pulmonary inflammation had an influence on NER activity. We found that in the lung the repair capacity was higher (~4-fold) in LPS-treated mice (Group II) than in controls (Group I) (Fig. 10A). More specifically, 2-way ANOVA of the log-transformed data indicated that pulmonary repair capacity was significantly increased following LPS-induced inflammation [$F(1,8) = 10.9$, $P = 0.0131$] (Group II) but was not further affected by BaP treatment (Groups III and IV). There was no significant interaction effect.

BaP treatment alone (Group III) had no effect on NER activity. Pulmonary repair capacities in the LPS (Group II) and LPS/BaP (Group IV) groups were similar to each other but not significantly different in the LPS/BaP group (Group IV) relative to controls (Group I) due to large inter-individual variability (Fig. 10A). In the liver no significant changes in NER capacity were observed between groups (Fig. 10B).

DISCUSSION

In the present study we have shown that pulmonary inflammation modulates the bioactivation of BaP and the concomitant respiratory tract DNA damage induced by it. To induce pulmonary inflammation we treated mice with LPS which is an established model to study non-allergic inflammation (Medan *et al.*, 2002; Gungor *et al.*, 2010a; Moriya *et al.*, 2012). The BaP dose used in this study (0.5 mg/mouse) has been shown to induce mutagenicity in the lung of *gpt* delta mice after a single intratracheal instillation (Hashimoto *et al.*, 2005). We found that BaP-induced DNA adduct formation in the lung was ~3-fold higher in LPS/BaP-treated mice compared to mice treated with BaP alone. Considering that inhaled combustion derived particles such as cigarette smoke, ambient air particulate matter and diesel exhaust particles contribute to pulmonary inflammation in humans (Kelly and Fussell, 2011) our results demonstrate that pulmonary inflammation could be a critical determinant in the induction of genotoxicity in the lung by particle-bound PAHs like BaP.

Pulmonary inflammation induced by LPS initiates the synthesis of pro-inflammatory cytokines (Gungor *et al.*, 2010b; Holand *et al.*, 2014). It has been shown that LPS-induced expression of cytokines like TNF-α and interleukin (IL)-1β in the liver is associated with altered *CYP* gene expression and CYP enzymes activities during inflammation (Warren *et al.*, 1999). In particular, it has been observed that *Cyp1a1* gene expression is suppressed by LPS and TNF-α in mouse liver and that activation of the nuclear factor-κB (NF-κB) plays an important role in *Cyp1a1* suppression (Ke *et al.*, 2001; Zordoky and El-Kadi, 2009). LPS-mediated decrease of hepatic Cyp1a1 was enhanced and accelerated in mice that lack the aryl hydrocarbon receptor (AhR) (*i.e. AhR(-/-)* mice) compared to *AhR(+/+)* mice (Wu *et al.*, 2011). Others have shown that enhanced expression of AhR in the thymus of LPS-treated mice was accompanied by increased Cyp1a1 expression which could be repressed by inhibition of NF-κB (Vogel *et al.*, 2014). Further, induction of Cyp1a1 by LPS in the thymus

depended on functional AhR as shown in *AhR(-/-)* mice (Vogel *et al.*, 2014). Together these data show that there is a cross-talk between AhR and inflammatory response that can be critical for the expression of CYP1A1 (Vondracek *et al.*, 2011). However, the observed responses are complex and tissue-specific, but it is noteworthy that PAHs like BaP can induce *Cyp1a1* transcription through binding to AhR (Shimizu *et al.*, 2000; Wang *et al.*, 2011).

In the present study we found a clear induction of Cyp1a1 protein in the lungs after BaP treatment both alone and in combination with LPS. In contrast no change of pulmonary Cyp1a1 protein was observed after LPS treatment alone. Interestingly pulmonary Cyp1a1 enzyme activity was lower in LPS/BaP-treated mice than in mice treated with BaP alone suggesting that pulmonary inflammation impacted on BaP-induced Cyp1a1 enzyme activity in the lung. Because BaP-DNA adduct levels in the lung were increased in LPS/BaP-treated mice compared to BaP-treated mice this observation may appear puzzling at first. However, previous studies (Arlt *et al.*, 2008; Arlt *et al.*, 2012; Nebert *et al.*, 2013) have revealed a paradox, whereby CYP enzymes (particularly CYP1A1) appear to be more important for detoxification of BaP *in vivo*, despite being involved in its metabolic activation *in vitro*. Therefore, the decrease in pulmonary Cyp1a1 enzyme activity in LPS/BaP-treated mice relative to BaP-treated mice, as measured in pulmonary microsomes, led to a decrease in BaP detoxification, thereby enhancing BaP genotoxicity (*i.e.* DNA adduct formation) in the lung. It remains to be investigated how pulmonary inflammation really impacts on Cyp1a1 enzyme activity but not Cyp1a1 protein expression (see below). Some other studies have suggested that CYP1B1 could play a role in the bioactivation of BaP within inflamed tissue as CYP1B1 can be up-regulated by proinflammatory cytokines (*i.e.* TNF-α) in BaP-treated cells *in vitro* and thus may redirect BaP metabolism to form higher amounts of BPDE and to potentiate DNA adduct formation (Umannova *et al.*, 2008; Smerdova *et al.*, 2013; 2014). However,

Cyp1b1 gene expression and Cyp1b1 protein analysis in the lung provided no evidence for an impact of pulmonary inflammation on Cyp1b1-mediated BaP bioactivation *in vivo*.

One mediator that may be involved in the suppression of pulmonary Cyp1a1 enzyme activity after LPS challenge could be the formation of reactive oxygen species (ROS) (Morel and Barouki, 1999). In this context it is noteworthy that CYP1A1 can produce ROS during its catalytic cycle (Morel and Barouki, 1999). It has been shown not only that LPS results in increased ROS production but also that ROS suppresses CYP1A1 expression in cultured human cells *in vitro* (Morel and Barouki, 1998). Therefore, it has been proposed that ROS such as hydrogen peroxide are involved in haemoprotein inactivation followed by haem loss (Karuzina and Archakov, 1994a; Karuzina and Archakov, 1994b). Similarly, BaP *o*-quinones formed during BaP metabolism have been shown to generate ROS (Park *et al.*, 2009). Other potential mechanisms might involve the modification of certain amino acids at or near the active centre of the CYP1A1 enzyme by hydrogen peroxide (Karuzina and Archakov, 1994b). Importantly, inactivated Cyp1a1 protein will retain the epitope for its recognition when assayed by Western blot analysis (El-Kadi *et al.*, 2000) but Cyp1a1 enzyme activity will be lost. Therefore, despite the induction of pulmonary Cyp1a1 protein, as measured by Western blotting in the LPS/BaP-treated mice, we propose that ROS formation leads to an inhibition of Cyp1a1 enzyme activity under the present experimental conditions.

If BaP is detoxified more slowly by Cyp1a1 in the lungs of LPS/BaP-treated mice, it would be predicted that more BaP circulates via the blood to extra-pulmonary tissues in these mice relative to mice treated with BaP alone. Indeed we observed higher BaP-DNA adduct levels in the livers of LPS/BaP-treated mice compared with BaP-treated mice. Further, it would be predicted that if in LPS/BaP-treated mice more BaP is transported from the lung via the blood to the liver than in BaP-treated mice, induction of Cyp1a1 protein and Cyp1a1 enzyme activity should be higher in the livers of LPS/BaP-treated mice relative to mice

treated with BaP alone. Indeed we found Cyp1a1 protein induction as well as an increase in Cyp1a1 enzyme activity in the livers of LPS/BaP-treated mice compared with BaP-treated mice, as measured in hepatic microsomes. Thus it would appear that a higher circulation of BaP to the liver results in higher DNA adduct levels, overriding the tendency of increased Cyp1a1 enzyme activity to result in a greater capacity to detoxify BaP. Our results suggest a dual role of Cyp1a1 in both bioactivation and detoxification of BaP *in vivo*. Similarly a dual role of CYP1A1 has been shown in the metabolism of the plant carcinogen aristolochic acid I (AAI) where CYP1A1 is able to catalyse the reductive activation of AAI to *N*-hydroxyaristolactam I and the oxidative detoxification to 8-hydroxyaristolochic acid (Stiborova *et al.*, 2012; 2014). These results in the liver also indicate that the presence of acute inflammation in one organ (*i.e.* lung) can influence the bioavailability of PAHs like BaP in other organs (*i.e.* liver) suggesting a systemic effect.

LPS-induced pulmonary inflammation also impacted on the expression of other xenobiotic-metabolising enzymes such as Nqo1 which may be important as BaP derivatives can be metabolised by NQO1 (Joseph and Jaiswal, 1994; Joseph and Jaiswal, 1998; Shen *et al.*, 2010). We found that Nqo1 enzyme activity was increased in the lung, after LPS and BaP treatment both alone and in combination. This may be critical for the bioactivation of diesel exhaust particle-bound nitro-PAHs as NQO1 has been shown to be a key enzyme in the metabolic activation of nitro-PAHs (Purohit and Basu, 2000; Stiborova *et al.*, 2010). Interestingly, pulmonary Nqo1 enzyme activity was decreased in LPS/BaP-treated mice relative to BaP-treated mice suggesting that the bioactivation of nitro-PAHs would be suppressed in these animals.

NER is considered to be the main DNA repair pathway for bulky DNA adducts (Friedberg, 2001). Using a modified comet assay we showed that tissue-specific NER capacity did not contribute to the higher BaP-DNA adduct levels observed in LPS/BaP-

treated mice than in BaP-treated mice in either lung or liver. LPS treatment led to a significant increase (~4-fold) in NER capacity in the lung. In contrast, Gungor and coworkers (Gungor *et al.*, 2010a) found that LPS exposure reduced NER capacity in lung tissue homogenate by ~50%. Although the LPS dose used was the same in both studies the discrepancy between the two studies might be attributable to the different LPS administration regimes (intratracheal instillation *versus* intranasal administration) but otherwise it remains unexplained at present.

In summary we found that pulmonary inflammation can impact on enzymes (*e.g.* CYPs) involved the activation and detoxification of PAHs. Our findings suggest that inflammatory signals and carcinogenic PAHs like BaP may interact and that LPS-induced pulmonary inflammation inhibits Cyp1a1 enzyme activity, which leads to increased DNA damage through the enhanced formation of covalent BaP-DNA adducts in the lungs *in vivo*. Thus pulmonary inflammation could be a critical contributor to the induction of genotoxicity by particle-bound PAHs in the lung.

FUNDING

Work at King's College London is supported by Cancer Research UK (Grant C313/A14329) and the Wellcome Trust (Grants 101126/Z/12/Z and 101126/B/13/Z). Annette Krais was supported by a fellowship from the German Research Foundation (DFG). Work at Charles University was supported by the Czech Science Foundation (Grant 15-02328S). Charmaine Corbin was supported by the MSc Programme in Biomedical and Molecular Sciences Research at King's College London. Quan Shi is supported by a personal grant from the Chinese Scholarship Council (CSC).

REFERENCES

Arlt, V. M., Stiborova, M., Henderson, C. J., Thiemann, M., Frei, E., Aimova, D., Singh, R., Gamboa da Costa, G., Schmitz, O. J., Farmer, P. B., Wolf, C. R., and Phillips, D. H. (2008). Metabolic activation of benzo[a]pyrene in vitro by hepatic cytochrome P450 contrasts with detoxification in vivo: experiments with hepatic cytochrome P450 reductase null mice. *Carcinogenesis* **29**, 656-665.

Arlt, V. M., Zuo, J., Trenz, K., Roufosse, C. A., Lord, G. M., Nortier, J. L., Schmeiser, H. H., Hollstein, M., and Phillips, D. H. (2011). Gene expression changes induced by the human carcinogen aristolochic acid I in renal and hepatic tissue of mice. *Int. J. Cancer* **128**, 21-32.

Arlt, V. M., Poirier, M. C., Sykes, S. E., John, K., Moserova, M., Stiborova, M., Wolf, C. R., Henderson, C. J., and Phillips, D. H. (2012). Exposure to benzo[a]pyrene of Hepatic Cytochrome P450 Reductase Null (HRN) and P450 Reductase Conditional Null (RCN) mice: Detection of benzo[a]pyrene diol epoxide-DNA adducts by immunohistochemistry and 32P-postlabelling. *Toxicol. Lett.* **213**, 160-166.

Attfield, M. D., Schleiff, P. L., Lubin, J. H., Blair, A., Stewart, P. A., Vermeulen, R., Coble, J. B., and Silverman, D. T. (2012). The Diesel Exhaust in Miners Study: A cohort mortality study with emphasis on lung cancer. *J. Natl. Cancer Inst.* **104**, 869-883.

Baird, W. M., Hooven, L. A., and Mahadevan, B. (2005). Carcinogenic polycyclic aromatic hydrocarbon-DNA adducts and mechanism of action. *Environ. Mol. Mutagen.* **45**, 106-114.

Borm, P. J., Knaapen, A. M., Schins, R. P., Godschalk, R. W., and Schooten, F. J. (1997). Neutrophils amplify the formation of DNA adducts by benzo[a]pyrene in lung target cells. *Environ. Health Perspect.* **105 Suppl 5**, 1089-1093.

Brody, J. S., and Spira, A. (2006). State of the art. Chronic obstructive pulmonary disease, inflammation, and lung cancer. *Proc. Am. Thorac. Soc.* **3**, 535-537.

El-Kadi, A. O., Bleau, A. M., Dumont, I., Maurice, H., and du Souich, P. (2000). Role of reactive oxygen intermediates in the decrease of hepatic cytochrome P450 activity by serum of humans and rabbits with an acute inflammatory reaction. *Drug Metab Dispos.* **28**, 1112-1120.

Friedberg, E. C. (2001). How nucleotide excision repair protects against cancer. *Nature Rev.* **1**, 22-33.

Grivennikov, S. I., Greten, F. R., and Karin, M. (2010). Immunity, inflammation, and cancer. *Cell* **140**, 883-899.

Gungor, N., Haegens, A., Knaapen, A. M., Godschalk, R. W., Chiu, R. K., Wouters, E. F., and van Schooten, F. J. (2010a). Lung inflammation is associated with reduced pulmonary nucleotide excision repair in vivo. *Mutagenesis* **25**, 77-82.

Gungor, N., Pennings, J. L., Knaapen, A. M., Chiu, R. K., Peluso, M., Godschalk, R. W., and Van Schooten, F. J. (2010b). Transcriptional profiling of the acute pulmonary inflammatory response induced by LPS: role of neutrophils. *Respir. Res.* **11**, 24.

Hashimoto, A. H., Amanuma, K., Hiyoshi, K., Takano, H., Masumura, K., Nohmi, T., and Aoki, Y. (2005). In vivo mutagenesis induced by benzo[a]pyrene instilled into the lung of gpt delta transgenic mice. *Environ. Mol.Mutagen.* **45**, 365-373.

Holand, T., Riffo-Vasquez, Y., Spina, D., O'Connor, B., Woisin, F., Sand, C., Marber, M., Bacon, K. B., Rohlff, C., and Page, C. P. (2014). A role for mitogen kinase kinase 3 in pulmonary inflammation validated from a proteomic approach. *Pulm. Pharmacol. Ther.* **27**, 156-163.

IARC (2010). Some non-heterocyclic polycyclic aromatic hydrocarbons and some related exposures. *IARC Monogr Eval Carcinog Risk Hum* **92**.

IARC (2013). Diesel and gasoline engine exhaust and some nitroarenes. *IARC Monogr Eval Carcinog Risk Hum* **105**.

Joseph, P., and Jaiswal, A. K. (1998). NAD(P)H:quinone oxidoreductase 1 reduces the mutagenicity of DNA caused by NADPH:P450 reductase-activated metabolites of benzo(a)pyrene quinones. *Br. J. Cancer* **77**, 709-719.

Joseph, P., and Jaiswal, A. K. (1994). NAD(P)H:quinone oxidoreductase$_1$ (DT diaphorase) specifically prevents the formation of benzo[a]pyrene quinone-DNA adducts generated by cytochrome P4501A1 and P450 reductase. *Proc. Natl. Acad. Sci. USA* **91**, 8413-8417.

Karuzina, I. I., and Archakov, A. I. (1994a). Hydrogen peroxide-mediated inactivation of microsomal cytochrome P450 during monooxygenase reactions. *Free Radic. Biol. Med.* **17**, 557-567.

Karuzina, I. I., and Archakov, A. I. (1994b). The oxidative inactivation of cytochrome P450 in monooxygenase reactions. *Free Radic. Biol. Med.* **16**, 73-97.

Kelly, F. J., and Fussell, J. C. (2011). Air pollution and airway disease. *Clin. Exp. Allergy* **41**, 1059-1071.

Ke, S., Rabson, A. B., Germino, J. F., Gallo, M. A., and Tian, Y. (2001). Mechanism of suppression of cytochrome P-450 1A1 expression by tumor necrosis factor-alpha and lipopolysaccharide. *J. Biol. Chem.* **276**, 39638-39644.

Knaapen, A. M., Gungor, N., Schins, R. P., Borm, P. J., and Van Schooten, F. J. (2006). Neutrophils and respiratory tract DNA damage and mutagenesis: a review. *Mutagenesis* **21**, 225-236.

Krais, A. M., Mühlbauer, K.-R., Kucab, J. E., Chinbuah, H., Cornelius, M. G., Wei, Q.-X., Hollstein, M., Phillips, D. H., Arlt, V. M., and Schmeiser, H. H. (2015). Comparison

of the metabolic activation of environmental carcinogens in mouse embryonic stem cells and mouse embryonic fibroblasts. *Toxicol. In Vitro* **29**, 34-43.

Kucab, J. E., Phillips, D. H., and Arlt, V. M. (2012). Metabolic activation of diesel exhaust carcinogens in primary and immortalized human TP53 knock-in (Hupki) mouse embryo fibroblasts. *Environ. Mol. Mutagen.* **53**, 207-217.

Langie, S. A., Knaapen, A. M., Brauers, K. J., van Berlo, D., van Schooten, F. J., and Godschalk, R. W. (2006). Development and validation of a modified comet assay to phenotypically assess nucleotide excision repair. *Mutagenesis* **21**, 153-158.

Loomis, D., Grosse, Y., Lauby-Secretan, B., El Ghissassi, F., Bouvard, V., Benbrahim-Tallaa, L., Guha, N., Baan, R., Mattock, H., Straif, K., and International Agency for Research on Cancer Monograph Working Group, I. (2013). The carcinogenicity of outdoor air pollution. *Lancet Oncol.* **14**, 1262-1263.

Martin, F. L., Patel, II, Sozeri, O., Singh, P. B., Ragavan, N., Nicholson, C. M., Frei, E., Meinl, W., Glatt, H., Phillips, D. H., and Arlt, V. M. (2010). Constitutive expression of bioactivating enzymes in normal human prostate suggests a capability to activate pro-carcinogens to DNA-damaging metabolites. *Prostate* **70**, 1586-1599.

Medan, D., Wang, L., Yang, X., Dokka, S., Castranova, V., and Rojanasakul, Y. (2002). Induction of neutrophil apoptosis and secondary necrosis during endotoxin-induced pulmonary inflammation in mice. *J. Cell Physiol.* **191**, 320-326.

Mizerovska, J., Dracinska, H., Frei, E., Schmeiser, H. H., Arlt, V. M., and Stiborova, M. (2011). Induction of biotransformation enzymes by the carcinogenic air-pollutant 3-nitrobenzanthrone in liver, kidney and lung, after intra-tracheal instillation in rats. *Mutat.Res.* **720**, 34-41.

Morel, Y., and Barouki, R. (1999). Repression of gene expression by oxidative stress. *Biochem J.* **342 Pt 3**, 481-496.

Morel, Y., and Barouki, R. (1998). Down-regulation of cytochrome P450 1A1 gene promoter by oxidative stress. Critical contribution of nuclear factor 1. *J. Biol. Chem.* **273**, 26969-26976.

Moriya, N., Kataoka, H., Fujino, H., Nishikawa, J., and Kugawa, F. (2012). Effect of lipopolysaccharide on the xenobiotic-induced expression and activity of hepatic cytochrome P450 in mice. *Biol. Pharm. Bull.* **35**, 473-480.

Nebert, D. W., Shi, Z., Galvez-Peralta, M., Uno, S., and Dragin, N. (2013). Oral benzo[a]pyrene: understanding pharmacokinetics, detoxication, and consequences--Cyp1 knockout mouse lines as a paradigm. *Mol. Pharmacol.* **84**, 304-313.

Park, J. H., Mangal, D., Frey, A. J., Harvey, R. G., Blair, I. A., Penning, T.M. (2009) Aryl hydrocarbon receptor facilitates DNA strand breaks and 8-oxo-2'-deoxyguanosine formation by the aldo-keto reductase product benzo[a]pyrene-7,8-dione. *J. Biol. Chem.* **284**, 29725-29734.

Petruska, J. M., Mosebrook, D. R., Jakab, G. J., and Trush, M. A. (1992). Myeloperoxidase-enhanced formation of (+-)-trans-7,8-dihydroxy-7,8-dihydrobenzo[a]pyrene-DNA adducts in lung tissue in vitro: a role of pulmonary inflammation in the bioactivation of a procarcinogen. *Carcinogenesis* **13**, 1075-1081.

Phillips, D. H. (2005). *Macromolecular adducts as biomarkers of human exposure to polycyclic aromatic hydrocarbons*. In The Carcinogenic Effects of Polycyclic Aromatic Hydrocarbons (A. Luch, Ed.), pp. 137-169. Imperial College Press, London.

Phillips, D. H., and Arlt, V. M. (2007). The 32P-postlabeling assay for DNA adducts. *Nat. Protoc.* **2**, 2772-2781.

Phillips, D. H., and Arlt, V. M. (2014). 32P-postlabeling analysis of DNA adducts. *Methods Mol Biol.* **1105**, 127-138.

Purohit, V., and Basu, A. K. (2000). Mutagenicity of nitroaromatic compounds. *Chem.Res. Toxicol.* **13**, 673-692.

Schottenfeld, D., and Beebe-Dimmer, J. (2006). Chronic inflammation: a common and important factor in the pathogenesis of neoplasia. *CA Cancer J. Clin.* **56**, 69-83.

Schwarze, P. E., Totlandsdal, A. I., Lag, M., Refsnes, M., Holme, J. A., and Ovrevik, J. (2013). Inflammation-related effects of diesel engine exhaust particles: studies on lung cells in vitro. *BioMed Res.Int.* **2013**, 685142.

Shen, J., Barrios, R. J., Jaiswal, A. K. (2010). Inactivation of the Quinone Oxidoreductases NQO1 and NQO2 strongly elevates the incidence and multiplicity of chemically induced skin tumors. *Cancer Res.* **70**, 1006-1014.

Shimizu, Y., Nakatsuru, Y., Ichinose, M., Takahashi, Y., Kume, H., Mimura, J., Fujii-Kuriyama, Y., and Ishikawa, T. (2000). Benzo[a]pyrene carcinogenicity is lost in mice lacking the aryl hydrocarbon receptor. *Proc. Natl. Acad. Sci. USA* **97**, 779-782.

Silverman, D. T., Samanic, C. M., Lubin, J. H., Blair, A. E., Stewart, P. A., Vermeulen, R., Coble, J. B., Rothman, N., Schleiff, P. L., Travis, W. D., Ziegler, R. G., Wacholder, S., and Attfield, M. D. (2012). The Diesel Exhaust in Miners Study: A nested case-control study of lung cancer and diesel exhaust. *J. Natl. Cancer Inst.* **104**, 855-868.

Smerdova, L., Neca, J., Svobodova, J., Topinka, J., Schmuczerova, J., Kozubik, A., Machala, M., Vondracek, J. (2013) Inflammatory mediators accelerate metabolism of benzo[a]pyrene in rat alveolar type II cells: the role of enhanced cytochrome P450 1B1 expression.*Toxicology* **314**, 30-38.

Smerdova, L., Svobodova, J., Kabatkova, M., Kohoutek, J., Blazek, D., Machala, M., and Vondracek, J. (2014). Upregulation of CYP1B1 expression by inflammatory cytokines is mediated by the p38 MAP kinase signal transduction pathway. *Carcinogenesis* **35,** 2534-2543.

Stiborova, M., Dracinska, H., Hajkova, J., Kaderabkova, P., Frei, E., Schmeiser, H. H., Soucek, P., Phillips, D. H., and Arlt, V. M. (2006). The environmental pollutant and carcinogen 3-nitrobenzanthrone and its human metabolite 3-aminobenzanthrone are potent inducers of rat hepatic cytochromes P450 1A1 and -1A2 and NAD(P)H:quinone oxidoreductase. *Drug Metab Dispos.* **34**, 1398-1405.

Stiborova, M., Martinek, V., Svobodova, M., Sistkova, J., Dvorak, Z., Ulrichova, J., Simanek, V., Frei, E., Schmeiser, H. H., Phillips, D. H., and Arlt, V. M. (2010). Mechanisms of the different DNA adduct forming potentials of the urban air pollutants 2-nitrobenzanthrone and carcinogenic 3-nitrobenzanthrone. *Chem. Res. Toxicol.* **23**, 1192-1201.

Stiborova, M., Levova, K., Barta, F., Shi, Z., Frei, E., Schmeiser, H. H., Nebert, D. W., Phillips, D. H., and Arlt, V. M. (2012) Bioactivation versus detoxication of the urothelial carcinogen aristolochic acid I by human cytochrome P450 1A1 and 1A2. *Toxicol. Sci.* **125**, 345-358.

Stiborova, M., Frei, E., Arlt, V.M., and Schmeiser, H. H. (2014) Knockout and humanized mice as suitable tools to identify enzymes metabolizing the human carcinogen aristolochic acid. *Xenobiotica* **44**, 135-145.

Stiborova, M., Barta, F., Levova, K., Hodek, P., Frei, E., Arlt, V. M., and Schmeiser, H. H. (2014). The influence of ochratoxin A on DNA adduct formation by the carcinogen aristolochic acid in rats. *Arch Toxicol.,* Sep 11. [Epub ahead of print].

Umannova, L., Machala, M., Topinka, J., Novakova, Z., Milcova, A., Kozubik, A., and Vondracek, J. (2008). Tumor necrosis factor-alpha potentiates genotoxic effects of benzo[a]pyrene in rat liver epithelial cells through upregulation of cytochrome P450 1B1 expression. *Mutat. Res.* **640**, 162-169.

Vogel, C. F., Khan, E. M., Leung, P. S., Gershwin, M. E., Chang, W. L., Wu, D., Haarmann-Stemmann, T., Hoffmann, A., and Denison, M. S. (2014). Cross-talk between aryl hydrocarbon receptor and the inflammatory response: a role for nuclear factor-kappaB. *J. Biol. Chem.* **289**, 1866-1875.

Vondracek, J., Umannova, L., and Machala, M. (2011). Interactions of the aryl hydrocarbon receptor with inflammatory mediators: beyond CYP1A regulation. *Curr. Drug Metab.* **12**, 89-103.

Walser, T., Cui, X., Yanagawa, J., Lee, J. M., Heinrich, E., Lee, G., Sharma, S., and Dubinett, S. M. (2008). Smoking and lung cancer: the role of inflammation. *Proc. Am. Thorac. Soc.* **5**, 811-815.

Wang, T., Gavin, H. M., Arlt, V. M., Lawrence, B. P., Fenton, S. E., Medina, D., and Vorderstrasse, B. A. (2011). Aryl hydrocarbon receptor activation during pregnancy, and in adult nulliparous mice, delays the subsequent development of DMBA-induced mammary tumors. *Int. J. Cancer* **128**, 1509-1523.

Warren, G. W., Poloyac, S. M., Gary, D. S., Mattson, M. P., and Blouin, R. A. (1999). Hepatic cytochrome P-450 expression in tumor necrosis factor-alpha receptor (p55/p75) knockout mice after endotoxin administration. *J. Pharmacol. Exp. Ther.* **288**, 945-950.

Wu, D., Li, W., Lok, P., Matsumura, F., and Vogel, C. F. (2011). AhR deficiency impairs expression of LPS-induced inflammatory genes in mice. *Biochem. Biophys. Res. Commun.* **410**, 358-363.

Zordoky, B. N., and El-Kadi, A. O. (2009). Role of NF-kappaB in the regulation of cytochrome P450 enzymes. *Curr. Drug Metab.* **10**, 164-178.

Table 1

Semi-quantitative assessment of pulmonary inflammation from H&E staining of lung sections

Treatment group (*n*= 4 per group)	% of fields with inflammation (median)	Size of inflammatory foci	Predominant cell type
Controls (Group I)	5-14 (6.5)	Small dense	Neutrophils
LPS (Group II)	26-92 (79)	Large loose	Monocytes
BaP (Group III)	4-32 (12.5)	Large loose	Monocytes
LPS+BaP (Group IV)	4-41 (18.5)	Large loose	Monocytes

Legends to figures

Figure 1

Main metabolic pathway in the bioactivation and DNA adduct formation of BaP in lung. See text for details. CYP, cytochrome P450; mEH, microsomal epoxide hydrolase; MPO, myleoperoxidase.Inserts: Autoradiographic profiles of DNA adducts in lungs formed in mice; the origin, at the bottom left-hand corner, was cut off before exposure. Autoradiographic profiles in the lungs are representative of those observed in the livers. The arrow shows 10-(deoxyguanosin-N^2-yl)-7,8,9-trihydroxy-7,8,9,10-tetrahydro-BaP (dG-N^2-BPDE).

Figure 2

Study design and animal treatment. See Materials & Methods for additional information.

Figure 3

Histological analysis of pulmonary inflammation. Representative photomicrographs of lung tissue section stained with H&E: (A) control mice: small sense foci of predominantly neutrophils; (B) LPS-, BaP- or LPS+BaP-treated lung: large loose foci of predominantly monocytes. Original magnification ×10, left panel; ×40, right panel. Semi-quantitative assessment of pulmonary inflammation is summarised in Table 1.

Figure 4

Effect of BaP treatment on pulmonary inflammation assessing bronchoalveolar lavage fluid. Total (A), neutrophil (B), mononuclear leukocytes (C) and eosinophil (D) cells were quantified by haemocytometry from mice treated with LPS, BaP, LPS+BaP or vehicle only (control). All values are given as the means ± SEM (n = 12 per group). In the figure F = fold

difference in cell number in LPS/BaP group compared with cell number in BaP group. Statistical analysis was performed by two-way ANOVA followed by Tukey's multiple comparisons test (*$P < 0.05$, *versus* control [untreated] mice; **$P < 0.05$, different BaP only treated mice).

Figure 5

BaP-DNA adduct formation. DNA adduct levels (RAL, relative adduct labelling) were measured by ^{32}P-postlabelling in lung (A) and liver (B) of mice treated with LPS, BaP, LPS+BaP or vehicle only (control). All values are given as the means ± SD ($n = 4$ per group). ND, not detected. In the figure F = fold difference in DNA binding in LPS/BaP group compared with DNA binding in BaP group. Statistical analysis was performed by unpaired two-tailed *t*-test (*$P < 0.05$, *versus* BaP only treated mice).

Figure 6

Western blot analysis of Cyp1a1 protein expression in lung (A) and liver (B) of mice treated with LPS, BaP, LPS+BaP or vehicle only (control). Representative images of the Western blotting are shown; duplicate analysis was performed on separate occasions. Gapdh protein expression was used as loading control.

Figure 7

Effect of BaP treatment on Cyp1a enzyme activity. Cyp1a1 enzyme activity as measured by EROD (A+C) or CEC activity (B+D) in microsomal fractions isolated from lung (A+B) or liver (C+D) tissues of mice treated with LPS, BaP, LPS+BaP or vehicle only (control). All values are given as the means ± SD of three separate determinations. RFU, relative fluorescence unit. ND, not detected. In the figure F = fold difference in enzyme activity in

LPS/BaP group compared with enzyme activity in BaP group. Statistical analysis was performed by unpaired two-tailed *t*-test ($^{*}P < 0.05$, *versus* BaP only treated mice).

Figure 8

Effect of BaP treatment on Nqo1 enzyme activity. Nqo1 enzyme activity was measured in cytosolic fractions isolated from lung (A) or liver (B) tissues of mice treated with LPS, BaP, LPS+BaP or vehicle only (control). All values are given as the means ± SD of three separate determinations. RFU, relative fluorescence unit. In the figure F = fold difference in enzyme activity in LPS/BaP group compared with enzyme activity in BaP group. Statistical analysis was performed by two-way ANOVA followed by Tukey's multiple comparisons test ($*P < 0.05$ *versus* control [untreated] mice; $^{**}P < 0.05$, *versus* BaP only treated mice).

Figure 9

Expression of Cyp1b1 in the lung of mice treated with LPS, BaP, LPS+BaP or vehicle only (control). (A) Gene expression of *Cyp1b1* assessed by RT-PCR. All values are given as the means ± SD ($n = 4$ per group). For statistical analysis the relative mRNA expression data was log2 transformed and analysed using a single sample *t*-test with Bonferroni correction against the population control mean of 0; no significant differences were observed. (B) Cyp1b1 protein expression determined by Western blot analysis. Representative images are shown; duplicate analysis was performed on separate occasions. Gapdh protein expression was used as loading control.

Figure 10

NER repair capacity was measured in tissue extracts isolated from lung (A) or liver (B) tissues of mice treated with LPS, BaP, LPS+BaP or vehicle only (control). All values are

given as the means ± SD (n = 3 per group). For statistical analysis the relative repair capacity data was log-transformed and analysed by two-way ANOVA followed by Sidak's multiple comparisons test (*$P < 0.05$, *versus* control [untreated] mice).

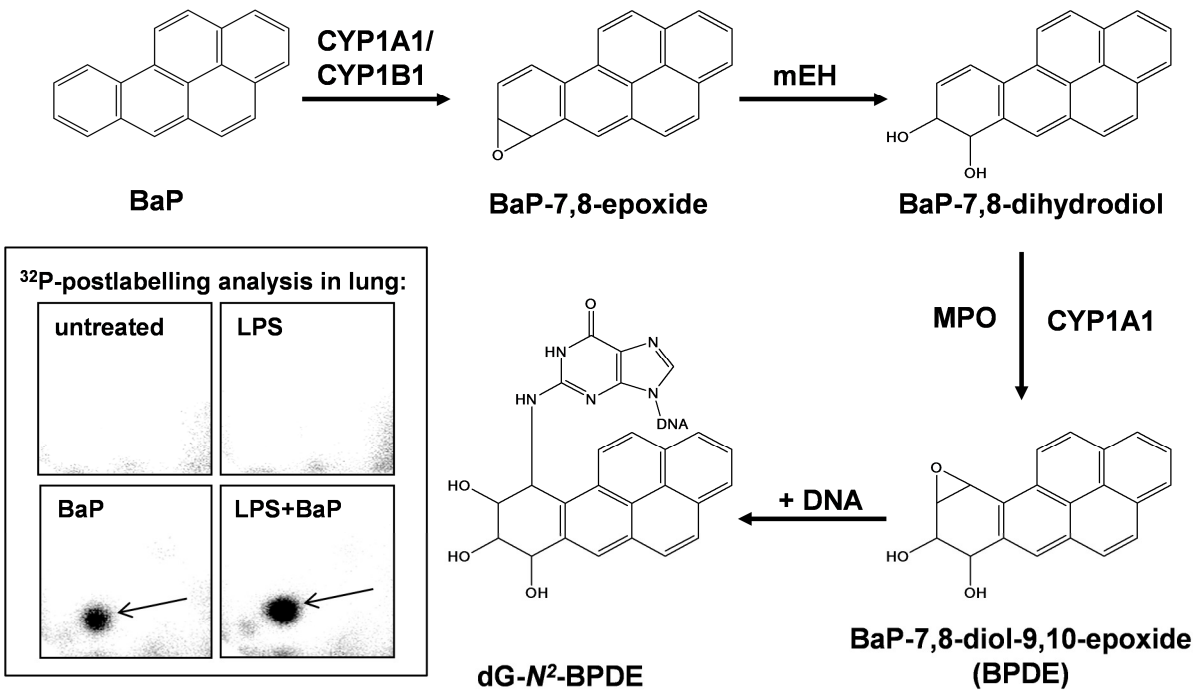
CYP1A1/
CYP1B1
mEH
BaP
BaP-7,8-epoxide
BaP-7,8-dihydrodiol
32P-postlabelling analysis in lung:
untreated
LPS
BaP
LPS+BaP
MPO
CYP1A1
+ DNA
DNA
BaP-7,8-diol-9,10-epoxide
(BPDE)
dG-N2-BPDE

Figure 1

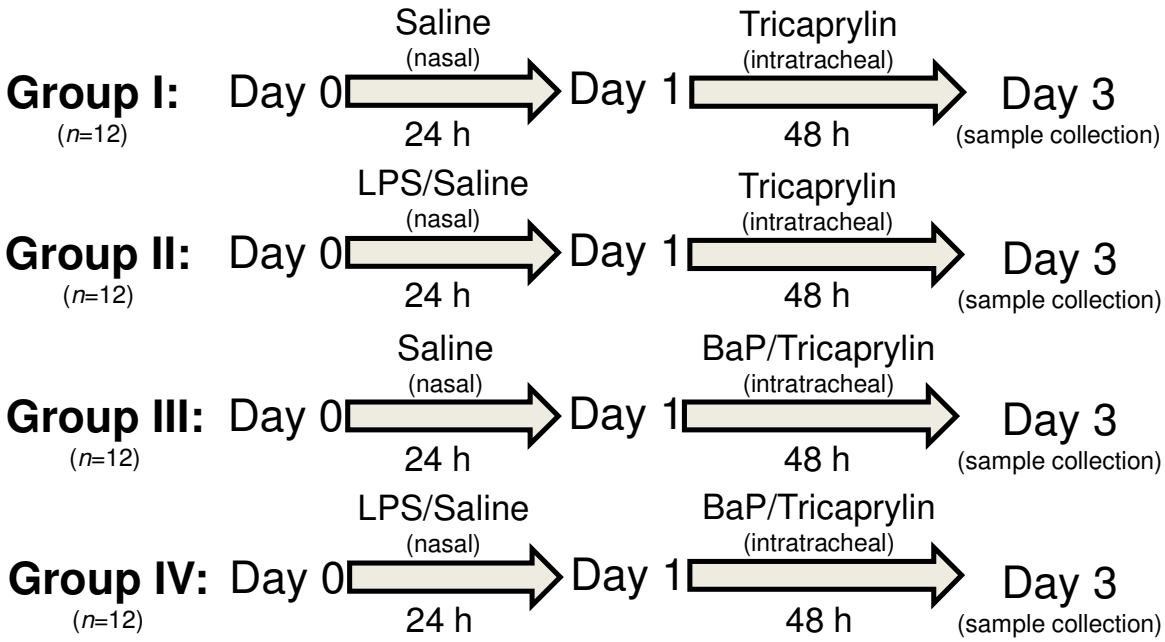
Group I:
(n=12)
Day 0
Saline
(nasal)
24 h
Day 1
Tricaprylin
(intratracheal)
48 h
Day 3
(sample collection)
Group II:
(n=12)
Day 0
LPS/Saline
(nasal)
24 h
Day 1
Tricaprylin
(intratracheal)
48 h
Day 3
(sample collection)
Group III:
(n=12)
Day 0
Saline
(nasal)
24 h
Day 1
BaP/Tricaprylin
(intratracheal)
48 h
Day 3
(sample collection)
Group IV:
(n=12)
Day 0
LPS/Saline
(nasal)
24 h
Day 1
BaP/Tricaprylin
(intratracheal)
48 h
Day 3
(sample collection)

Figure 2

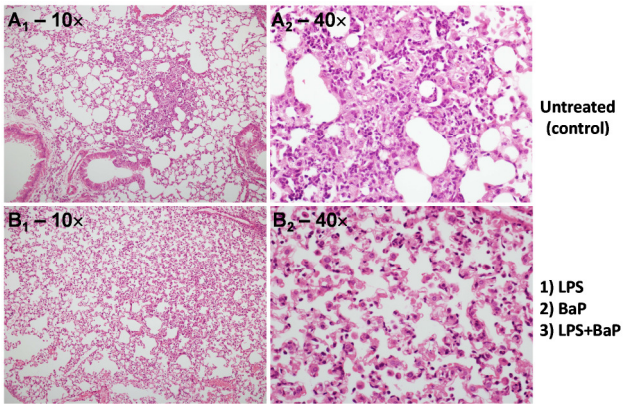

Figure 3

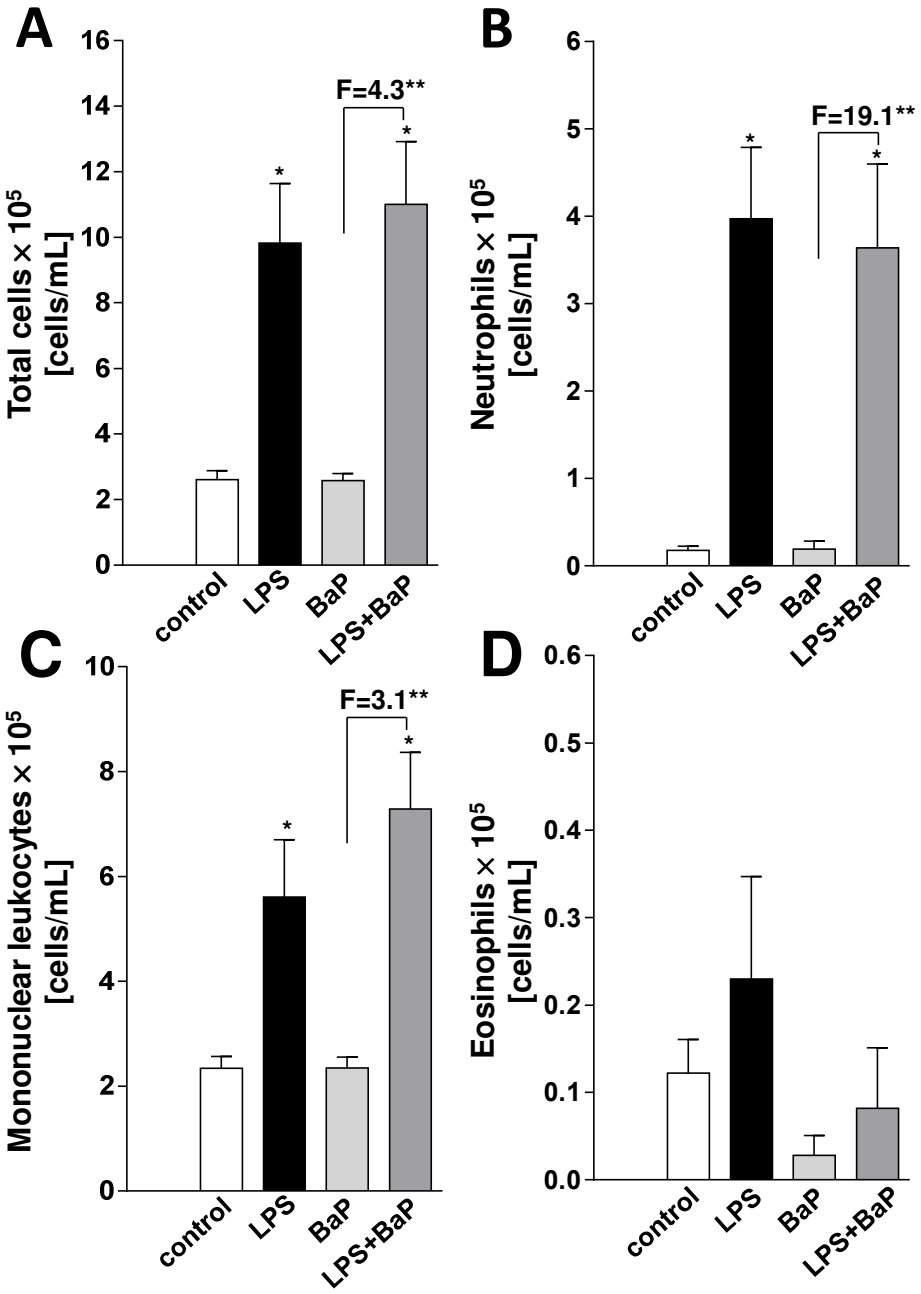
A
Total cells × 10⁵ [cells/mL]
F=4.3**
control
LPS
BaP
LPS+BaP
B
Neutrophils × 10⁵ [cells/mL]
F=19.1**
C
Mononuclear leukocytes × 10⁵ [cells/mL]
F=3.1**
D
Eosinophils × 10⁵ [cells/mL]

Figure 4

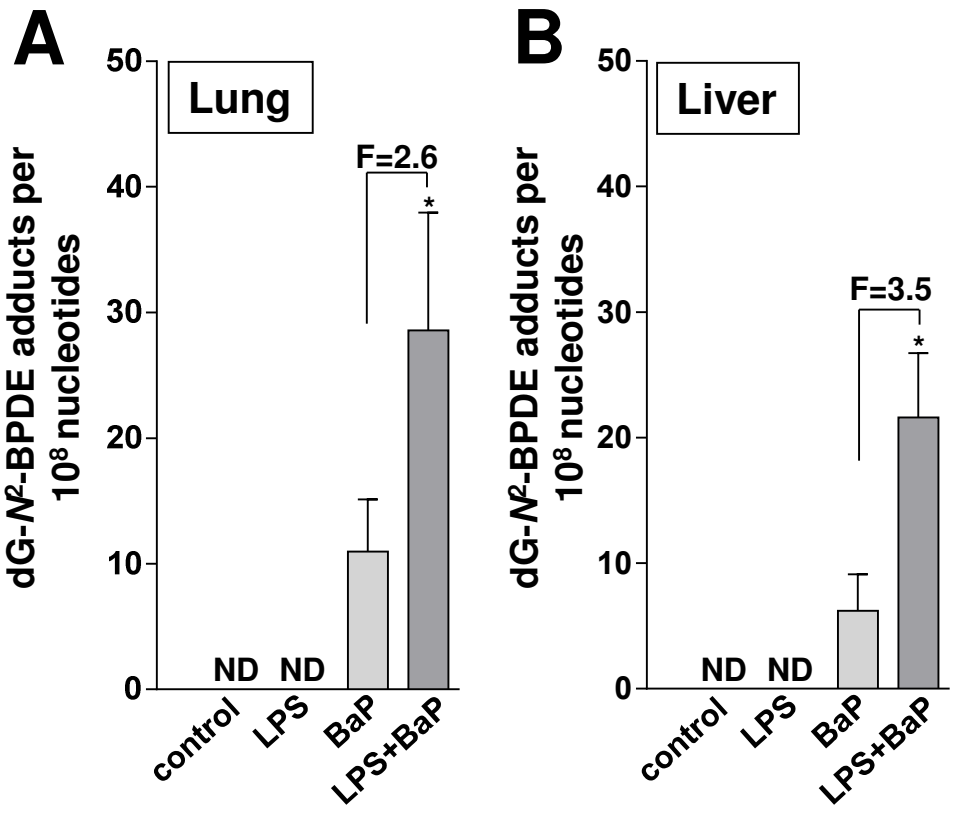
A
Lung
dG-N2-BPDE adducts per 10^8 nucleotides
50
40
30
20
10
0
F=2.6
*
ND
ND
control
LPS
BaP
LPS+BaP
B
Liver
dG-N2-BPDE adducts per 10^8 nucleotides
50
40
30
20
10
0
F=3.5
*
ND
ND
control
LPS
BaP
LPS+BaP

Figure 5

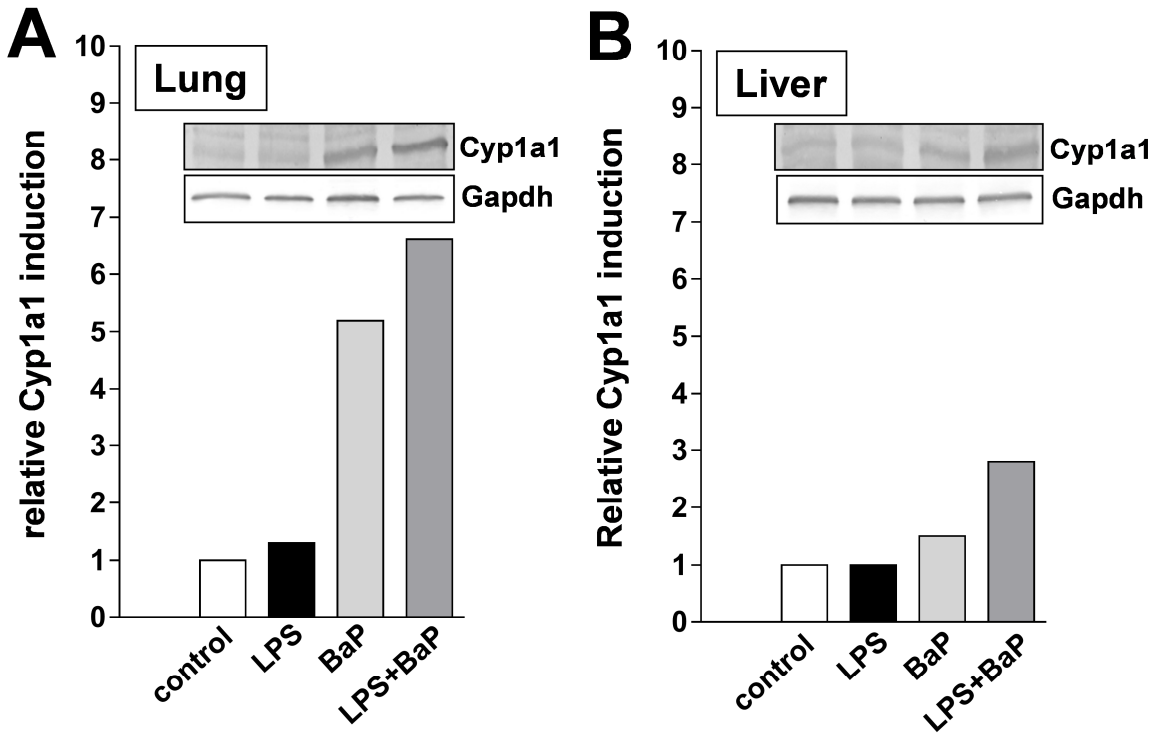
A
Lung
relative Cyp1a1 induction
10
9
8
7
6
5
4
3
2
1
0
Cyp1a1
Gapdh
control
LPS
BaP
LPS+BaP
B
Liver
Relative Cyp1a1 induction
Cyp1a1
Gapdh
control
LPS
BaP
LPS+BaP

Figure 6

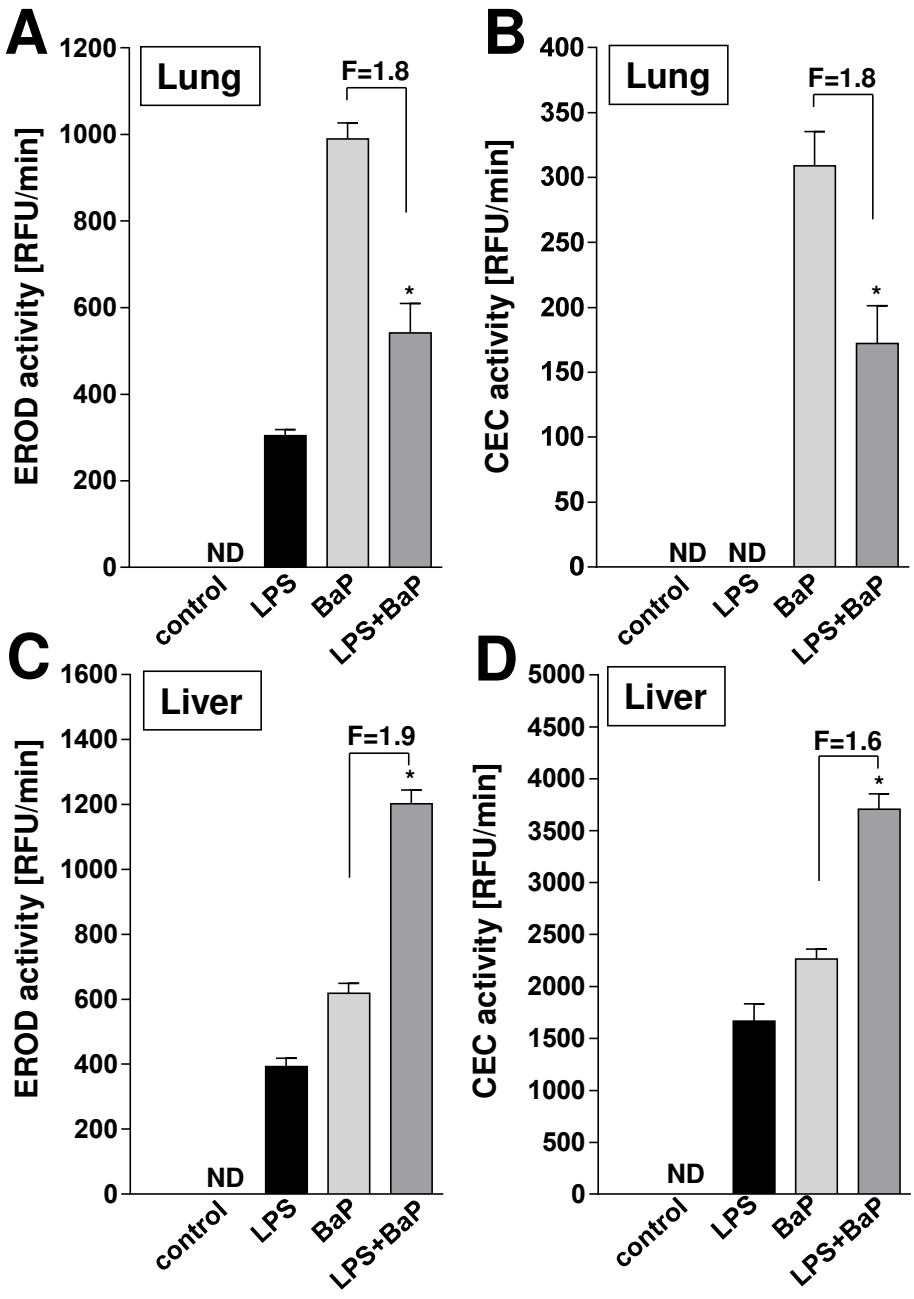
A
Lung
EROD activity [RFU/min]
F=1.8
ND
control
LPS
BaP
LPS+BaP
B
Lung
CEC activity [RFU/min]
F=1.8
ND
ND
C
Liver
EROD activity [RFU/min]
F=1.9
D
Liver
CEC activity [RFU/min]
F=1.6

Figure 7

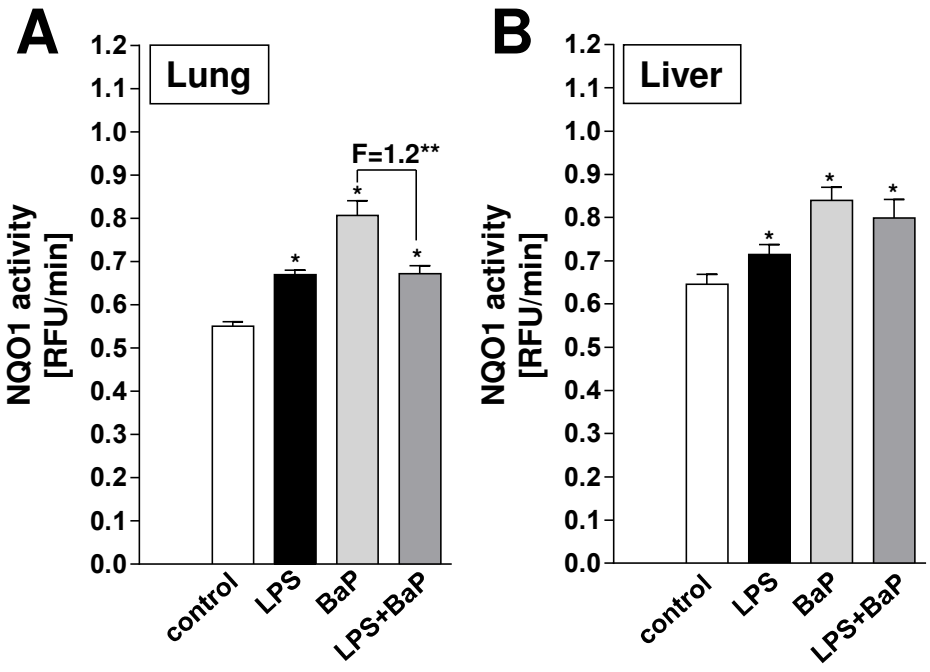
A
Lung
NQO1 activity [RFU/min]
1.2
1.1
1.0
0.9
0.8
0.7
0.6
0.5
0.4
0.3
0.2
0.1
0.0
F=1.2**
*
*
*
control
LPS
BaP
LPS+BaP
B
Liver
NQO1 activity [RFU/min]
1.2
1.1
1.0
0.9
0.8
0.7
0.6
0.5
0.4
0.3
0.2
0.1
0.0
*
*
*
control
LPS
BaP
LPS+BaP

Figure 8

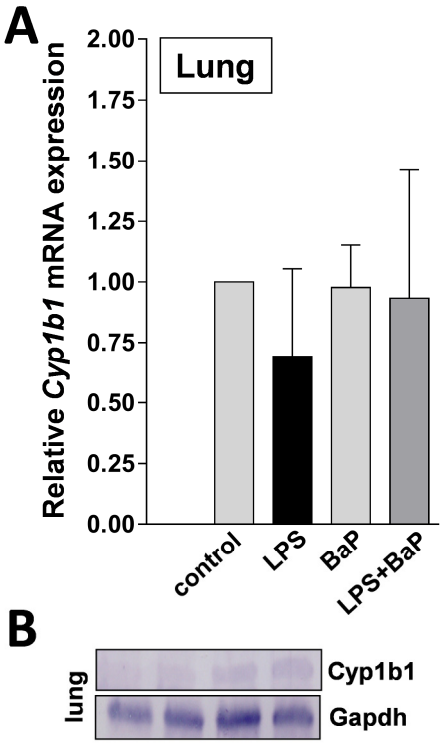
A
Lung
Relative Cyp1b1 mRNA expression
2.00
1.75
1.50
1.25
1.00
0.75
0.50
0.25
0.00
control
LPS
BaP
LPS+BaP
B
lung
Cyp1b1
Gapdh

Figure 9

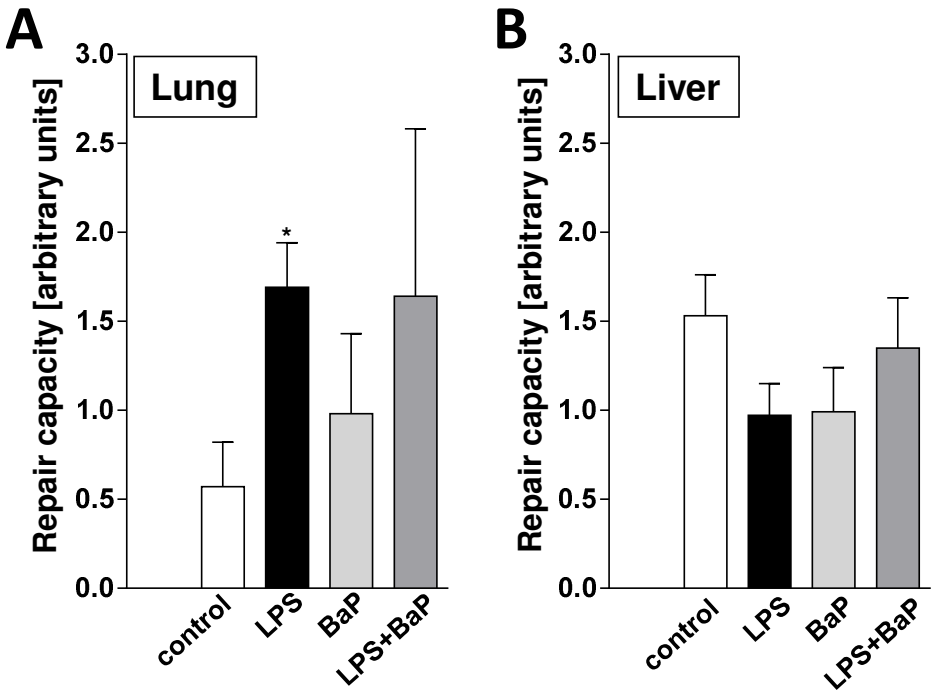
A
Lung
Repair capacity [arbitrary units]
3.0
2.5
2.0
1.5
1.0
0.5
0.0
*
control
LPS
BaP
LPS+BaP
B
Liver
Repair capacity [arbitrary units]
3.0
2.5
2.0
1.5
1.0
0.5
0.0
control
LPS
BaP
LPS+BaP

Figure 10